SANDIA REPORT

SAND2008-3871
Unlimited Release
Printed June 2008

THRIVE: a data reduction program for three-phase PDV/PDI and VISAR measurements

Daniel H. Dolan and Scott C. Jones

Prepared by
Sandia National Laboratories
Albuquerque, New Mexico 87185 and Livermore, California 94550

Sandia is a multiprogram laboratory operated by Sandia Corporation,
a Lockheed Martin Company, for the United States Department of Energy's
National Nuclear Security Administration under Contract DE-AC04-94-AL85000.

Issued by Sandia National Laboratories, operated for the United States Department of Energy by Sandia Corporation.

Available to DOE and DOE contractors from
U.S. Department of Energy
Office of Scientific and Technical Information
P.O. Box 62
Oak Ridge, TN 37831

Telephone: (865) 576-8401
Facsimile: (865) 576-5728
E-Mail: reports@adonis.osti.gov
Online ordering: http://www.osti.gov/bridge

Available to the public from
U.S. Department of Commerce
National Technical Information Service
5285 Port Royal Rd
Springfield, VA 22161

Telephone: (800) 553-6847
Facsimile: (703) 605-6900
E-Mail: orders@ntis.fedworld.gov
Online ordering: http://www.ntis.gov/help/ordermethods.asp?loc=7-4-0#online

SAND2008-3871
Unlimited Release
Printed June 2008

THRIVE: a data reduction program for three-phase PDV/PDI and VISAR measurements

Daniel H. Dolan and Scott C. Jones
Sandia National Laboratories
P.O. Box 5800
Albuquerque, NM 87185-1195

Abstract

THRIVE (THRee Interferometer VElocimetry) is an analysis package for reducing three-phase interferometry measurements. Three-phase displacement interferometry measurements are the primary application of this program, although velocity interferometry is also supported. THRIVE uses a push-pull approach to transform measured signals to a pair of quadrature signals, from which fringe shift, target position, and target velocity are inferred. The program can analyze the signals in an ideal sense or compensate for non-ideal measurement conditions using ellipse characterization. The program can be run in any current version of MATLAB (release 2007a or later) or as a Windows XP executable.

Acknowledgments

The THRIVE program builds upon discussions with several individuals. Bruce Marshall introduced the 3×3 coupler to the NNSA community, creating the need for three-phase data reduction. An earlier PDI analysis package by Andrew Sibley and Adrian Hughes stimulated work on a robust data reduction method, following the push-pull concept proposed by Will Hemsing for VISAR. Additional capabilities and features in the program were created in part due to conversation/debates with David Holtkamp and Mike Furnish.

Table of Contents

List of Figures

CHAPTER 1

Introduction

For decades, VISAR (Velocity Interferometer System for Any Reflector) [1] has been the primary time-resolved velocity diagnostic for shock wave experiments. A chief advantage of VISAR is that substantial velocities (> 1 km/s) can be tracked with modest diagnostic bandwidth. Displacement interferometry has been used in dynamic compression experiments [2], but the method was intrinsically limited by detector and digitizer speed.

Using high speed diagnostics and fiber optic hardware from the telecommunications industry, Strand *et. al* [3] built a compact displacement interferometer capable of tracking motion up to 5 km/s. Originally called heterodyne velocimetry, the technique is widely known as PDV or PDI[1] and is rapidly finding applications in dynamic compression research and various related fields. Operating in the near-infrared (1550 nm) rather than visible spectrum, PDV is essentially a fiber-based Michelson interferometer. Velocity is inferred by measuring the beat frequency produced by the interference of Doppler shifted light with an unshifted source.

Three-phase PDV systems have recently been constructed to resolve sub-fringe phenomena. This approach probes target position directly, rather than beat frequency, and is well suited to non-constant velocity measurements. Furthermore, three-phase measurements can discern the motion reversal, something that a single-phase measurement cannot do. Conceptually, data reduction of a three-phase PDV measurement is quite similar to a push-pull VISAR measurement. This report describes a program developed at Sandia National Laboratories to analyze three-phase PDV measurements.

1.1 Program summary

THRIVE (THRee Interferometer VElocimetry) is a program for reducing a set of three interferometer signals, nominally delayed by 120°. The program is primarily intended for three-phase PDV measurements, but can also be applied to velocity interferometers. Signal characterization capabilities are included in the program, allowing robust analysis in presence of various measurement imperfections. THRIVE uses a simple graphical interface to guide users through the analysis process.

[1] The terms Photonic Doppler Velocimetry (PDV) and Photonic Displacement Interferometry (PDI) describe the same diagnostic. The name "HetV" is also used in some settings.

THRIVE is written in MATLAB, and can operate on any platform where version 2007a or later is available (OS X, Linux, and Windows XP/Vista). A compiled executable is available for Windows XP for non-MATLAB users. The program can be obtained by contacting Scott Jones (`scjones@sandia.gov`).

1.2 Chapter organization

Chapter 2 gives a theoretical background for the THRIVE program, covering several aspects of the analysis. Chapter 3 presents a overview of the program's usage and capabilities. Chapter 4 gives more specific details about using THRIVE, including a complete analysis example. Chapter 5 describes a series of benchmark problems, highlighting salient program features. Chapter 6 summarizes the program's capabilities and discusses future releases.

CHAPTER 2

Theoretical background

This chapter reviews theoretical concepts used in the THRIVE program. First, the conceptual operation of displacement and velocity interferometers is presented. Next, three-phase interferometer measurements are described. Finally, numerical differentiation using the Savitzky-Golay approach is discussed.

2.1 Interferometry measurements

THRIVE analyzes data from both displacement and velocity interferometry measurements. Displacement configuration is used in PDV measurements, while the velocity configuration is used in VISAR measurements. The critical distinction between these configurations is how the output varies with target motion. In the velocity configuration, the measured output changes with the target's velocity, which means that constant velocity corresponds to a constant signal. This is not the case in the displacement configuration, where constant velocity yields a time varying signal.

A potentially confusing aspect of each measurement configuration is that the results can be *analyzed* in terms of the target displacement or velocity. Velocity analysis relies on the assumption of nearly constant motion over some intrinsic time scale; displacement analysis is the more rigorous approach, but may suffer from numerical difficulties. Both types of analysis are developed here for the displacement configuration. Reference 4 provides a complete discussion of the analysis of the velocity configuration, and only a brief summary is provided here.

2.1.1 Displacement configuration

Figure 2.1 shows the conceptual layout of a displacement interferometer. Coherent light input is split along two paths, one of which strikes a moving target at position $x(t)$. Doppler shifted light reflected by the target is combined with a reference signal (an unshifted portion of the input) at a reference position x_r and recorded with an optical detector. Interference between the two optical frequencies produces a beat frequency proportional to the target velocity.

To develop a precise relationship between target motion and measured detector signals, suppose that the optical intensity returning from the target is $I_T(t)$ and the reference intensity split off of

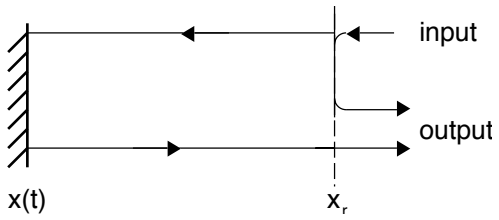

Figure 2.1. Displacement interferometer measurement

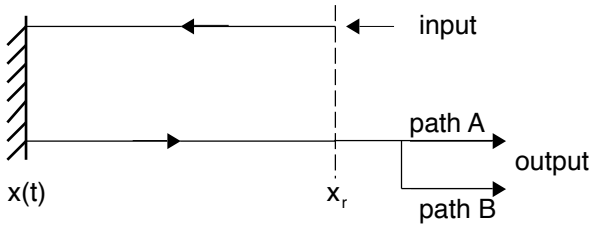

Figure 2.2. Velocity interferometer measurement

the input is I_R.[1] The output intensity is then:

$$I(t) = I_R + I_T(t) + 2\sqrt{I_R I_C(t)}\cos\Phi(t) \tag{2.1}$$

where $\Phi(t)$ is the optical phase difference [5], which describes the interference of light traveling along the two different paths. Optical phase difference is related to the target's position relative to a reference position at time t_i.

$$\Phi(t) = \Phi(t_i) + 4\pi\frac{x(t) - x(t_i)}{\lambda_0} \tag{2.2}$$

A detector recording the output intensity would yield the following electrical signal.

$$D(t) = aI_R + bI_T(t) + 2\sqrt{abI_R I_C(t)}\cos\underbrace{\left[\Phi(t_i) + 4\pi\frac{x(t) - x(t_i)}{\lambda_0}\right]}_{=2\pi f(t)} \tag{2.3}$$

The constants a and b represent a collection of coupling factors (from the reference and target paths, respectively) and the detector's sensitivity. The fringe shift $f(t)$ is the essential quantity relating target motion to the measured signal—each integer fringe increment indicates the target has moved half an optical wavelength. When the target moves with *constant* velocity v, the output signal has a beat frequency ν_b.

$$\nu_b = \frac{2v}{\lambda_0} \tag{2.4}$$

For example, a 1 km/s target velocity corresponds to a 1.29 GHz beat frequency for a 1550 nm input source.

The most basic analysis of a displacement interferometry measurement is to determine the target's position by counting fringes. Direct extraction of the fringe shift from a single channel is difficult, however, unless the signal has good contrast and nearly constant fringe amplitude. Furthermore, the measurement is insensitive to direction, so motion toward and away from the system at the same speed yields precisely the same signal. A related problem is that motion changes near a minimum or maximum of the detector signal are difficult to resolve.

More generally, time-frequency analysis is used to extract velocity from a displacement interferometry measurement. For example, a short time Fourier transform [6] can be used to extract spectrograms along different portions of the detector signal, the peaks of which correspond to velocities detected by the PDV system. References 3 and 5 demonstrate several examples of this technique. A major shortcoming of time-velocity analysis is that frequency measurements require a finite time window, usually several fringes. This limitation is quantitatively expressed by an uncertainty principle [5]:

$$(\delta v)\tau > \frac{\lambda_0}{8\pi} \tag{2.5}$$

where τ is the transform window size. The fractional velocity uncertainty is obtained by combining the above relation with Equation 2.4.

$$\frac{\delta v}{v} > \frac{1}{4\pi}\frac{T_b}{\tau} \qquad (T_b = 1/\nu_b) \tag{2.6}$$

[1] Throughout this work it is assumed that the reference intensity is constant and entirely coherent, while the target reflection may be time dependent and partially incoherent ($I_C < I_T$).

For a transform window precisely matched to the beat period T_b, the lowest possible velocity uncertainty is 8%; in practice, a much larger time resolution sacrifice will be required to obtain this velocity resolution. The uncertainty principle is particularly troublesome at low velocities, where the measured beat frequency may be slower than other features of interest.

2.1.2 Velocity configuration

Figure 2.2 shows the conceptual layout of what is often referred to as a velocity interferometer; strictly speaking, this is a differential displacement interferometer that approximates a velocity interferometer on sufficiently long time scales [4]. The key distinction between this configuration from a displacement interferometer is that the combined light contains two Doppler shifted signals, one time delayed from the other, rather than shifted and unshifted light. The sensitivity of a velocity interferometer can be controlled by varying the delay between paths A and B.

The signal measured by a velocity interferometer:

$$D(t) = aI_A(t) + bI_B(t) + 2\sqrt{abI_A(t)I_B(t)}\cos 2\pi f(t) \tag{2.7}$$

differs from a displacement interferometer measurement in several ways. First, the fringe shift is now directly proportional to target velocity:

$$f(t) \equiv \frac{\Phi(t) - \Phi(t_i)}{2\pi} \approx \frac{v}{K} \tag{2.8}$$

where the fringe constant K is related to the operating wavelength and interferometer delay [4]. Light intensity can vary in both legs of the interferometer instead of just one, though typically the time profiles of $I_A(t)$ and $I_B(t)$ are similar.

Velocity interferometers must deal with dynamic light conditions, incoherent light emission, and resolution difficulties near peaks/troughs of the detector signal. These challenges led to the development of the conventional [1] and push-pull [7] VISAR.

2.2 Three-phase measurements

An essential task in both displacement and velocity interferometer measurements is calculating the fringe shift for the motion under study. This operation should be performed in an unambiguous fashion with minimum human intervention. Such performance is impossible for a single channel displacement interferometer faced with a time varying velocity and motion reversals. A robust way of approaching this task is the use of balanced quadrature signals.

Figure 2.3 illustrates how quadrature can be obtained in a fiber based displacement interferometer; similar measurements can be made with a velocity interferometer [8]. The key component, the 3×3 fiber coupler, provides signal outputs phase shifted by roughly 120° [9]. A robust analysis [10] can be used to determine the fringe shift directly.[2] Three detector signals are reduced to a pair of ideal quadrature signals. If done correctly, this reduction can effectively deal with common measurement imperfections.

[2]This discussion assumes the measurement contains a single fringe shift, not a collection of superimposed fringes. Superimposed fringe patterns will cause contrast difficulties similar to that observed in VISAR [4] and require time-frequency analysis.

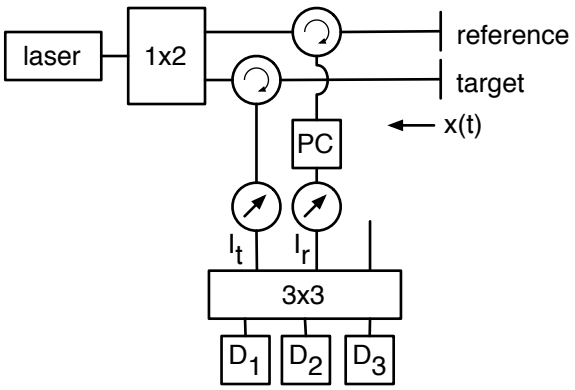

Figure 2.3. Three-phase PDV measurement. Two optical signals are sent into a 3×3 fiber coupler; the third input is not used. Phase shifted outputs obtained from the fiber coupler are recorded by separate detectors for quadrature reduction.

2.2.1 Principles

The output signals of a three-phase measurement have the form:

$$D_k(t) = \underbrace{a_k I_R + b_k I_T(t)}_{B_k(t)} + \underbrace{2\sqrt{a_k b_k I_R I_C((t)}}_{A_k(t)} \cos\left[\Phi(t) - \beta_k\right] \tag{2.9}$$

where $k = 1, 2, 3$ and β_k is the relative phase delay of the k-th signal. The second signal is assumed to lead the first by a phase β_+ ($\beta_2 = -\beta_+$), while the third signal lags the first by a phase β_- ($\beta_3 = \beta_-$); the phase shift of the first signal is incorporated into the definition of Φ. The values of β_+ and β_- are approximately 120°, though 10–20° variations are not unexpected [11].

The first two terms in Equation 2.9 comprise the signal baseline $B_k(t)$, while $A_k(t)$ is the signal amplitude. For constant and completely coherent target intensity $\bar{I}_T$, the detector signals have characteristic baselines $\bar{B}_k$ and amplitudes $\bar{A}_k$, suggesting the following normalization.

$$\tilde{D}_k(t) \equiv \frac{D_k(t) - \bar{B}_k}{\bar{A}_k} = \frac{1}{2}\sqrt{\frac{b_k}{a_k}}\frac{I_T(t) - \bar{I}_T}{\sqrt{I_R \bar{I}_C}} + \sqrt{\frac{I_C(t)}{\bar{I}_C}}\cos\left(\Phi(t) - \beta_k\right) \tag{2.10}$$

The target and coherent intensities can be eliminated by considering the ratio of scaled signal differences:

$$\frac{\tilde{D}_1(t) - R_{12}\tilde{D}_2(t)}{\tilde{D}_1(t) - R_{13}\tilde{D}_3(t)} = \frac{\cos\Phi(t) - R_{12}\cos(\Phi(t) + \beta_+)}{\cos\Phi(t) - R_{13}\cos(\Phi(t) - \beta_-)}$$

where $R_{12} = \sqrt{a_2/a_1}\sqrt{b_1/b_2}$ and $R_{13} = \sqrt{a_3/a_1}\sqrt{b_1/b_3}$. The above expression leads to a pair of quadrature signals, D_x and D_y, exactly 90° out of phase.

$$\tan\Phi(t) = \frac{\sum_{k=1}^{3} g_k \tilde{D}_k(t)}{\sum_{k=1}^{3} h_k \tilde{D}_k(t)} = \frac{D_y(t)}{D_x(t)} \tag{2.11}$$

$$\begin{aligned} g_1 &= R_{12}\cos\beta_+ - R_{13}\cos\beta_- & h_1 &= R_{12}\sin\beta_+ + R_{13}\sin\beta_- \\ g_2 &= -R_{12} + R_{12}R_{13}\cos\beta_- & h_2 &= -R_{12}R_{13}\sin\beta_- \\ g_3 &= +R_{13} - R_{12}R_{13}\cos\beta_+ & h_3 &= -R_{12}R_{13}\sin\beta_+ \end{aligned}$$

Each quadrature signal is a weighted sum of the normalized detector signals.

Using Equation 2.11, the three measured signals can be reduced to a pair of quadrature signals, which are then transformed into a fringe shift $f(t)$ via careful evaluation of the inverse tangent function. Target position is related to the fringe shift by the operating wavelength.

$$x(t) = x(t_i) + \frac{\lambda_0}{2} f(t) \tag{2.12}$$

Target velocity is determined by numerical differentiation of the fringe shift.

$$v(t) = \frac{\lambda_0}{2}\frac{df(t)}{dt} \tag{2.13}$$

2.2.2 Ellipse characterization

For a perfect PDV system, where the signals are exactly 120° and recorded by identical detectors, the quadrature relation reduces to the following form [12].

$$\tan\Phi(t) = \sqrt{3}\frac{D_3 - D_2}{2D_1 - D_2 - D_3} \tag{2.14}$$

The ideal state requires no system characterization, and the recorded signals $D_k(t)$ can be used without normalization. In general, a PDV measurement is characterized by four system parameters (R_{12}, R_{13}, β_+, β_-), three reference baselines ($\bar{B_k}$), and three reference amplitudes ($\bar{A_k}$). Together, there are ten individual parameters in a PDV measurement, but several of these parameters are interrelated.

Consider a set of ellipse fits to signal pairs $D_2 - D_1$ and $D_3 - D_1$.

$$\begin{aligned} D_1 &= B_1 + A_1\cos\Phi \\ D_j &= B_j + A_j\cos(\Phi - \beta_j) \qquad j = 2,3 \end{aligned}$$

The parameters for each ellipse yield the characteristic baselines, characteristic amplitudes, and phase shifts ($\beta = \epsilon + 90°$). The scaling parameters R_{12} and R_{13} are given by:

$$R_{1j} = \left(\frac{1 \pm_j \sqrt{1 - C_j^2}}{1 \pm_1 \sqrt{1 - C_1^2}} \times \frac{1 \mp_1 \sqrt{1 - C_1^2}}{1 \mp_j \sqrt{1 - C_j^2}}\right)^{1/2} \tag{2.15}$$

where $C_k = \bar{A}_k/\bar{B}_k$ (signal contrast). There are eight possible parameter combinations (corresponding to three root sign choices) for a given set of ellipses. This ambiguity can be resolved by asserting whether each detector receives more light from the reference or the target. Similar behavior is expected for all three channels, reducing parameter ambiguity from eight to two possibilities.

The baselines and amplitudes are a function of the individual detector sensitivities, and must be characterized if any of these components are changed. The remaining four parameters (R_{12}, R_{13}, β_+, and β_-), however, are dictated by the 3×3 coupler, not detector sensitivity. As such, it may be possible to characterize some aspects of a three-phase PDV system independently of the detectors. For example, inline power meters could be used to infer R_{12} and R_{13} using the definitions on page 14.

2.2.3 AC coupling

The ellipse characterization described above must be modified for AC coupled measurements, where static portions of the signal (such as the reference intensity) are eliminated from the measurement. To illustrate this point, consider a three-phase PDV measurement for which the target is stationary and the target intensity (total and coherent portion) are constant prior to initial time t_i. For ideal AC coupling, where the cutoff frequency is much lower than beat frequencies of interest,

the recorded signals can be expressed as follows.

$$\begin{aligned} F_k(t) &= D_k(t) - D_k(t_i) \\ &= b_k \left(I_T(t) - I_T(t_i) \right) - 2\sqrt{a_k b_k I_R I_C(t_i)} \cos\left(\Phi(t_i) - \beta_k\right) \\ &\quad + 2\sqrt{a_k b_k I_R I_C(t)} \cos\left(\Phi(t) - \beta_k\right) \end{aligned}$$

The first two terms of the AC coupled signal can drop below zero and lead to unphysical contrast values based on the preceding analysis.

Suspending the requirement that the ellipse fits lead to the scaling ratios R_{1j} (Equation 2.15), signal normalization remains useful in AC coupled measurements as long as an ellipse can be fit to a region of constant target intensity and coherence (quantities denoted with a bar).

$$\begin{aligned} \tilde{F}(t) &= \frac{F_k(t) - B_k}{A_k} \\ &= \sqrt{\frac{b_k}{a_k}} \frac{I_T(t) - \bar{I}_T}{2\sqrt{I_R \bar{I}_C}} + \sqrt{\frac{I_C(t)}{\bar{I}_C}} \cos\left(\Phi(t) - \beta_k\right) \end{aligned} \tag{2.16}$$

Following the logic from Section 2.2.1, this expression can be reduced to a pair of quadrature signals (Equation 2.11). The only remaining difficulty is determining the coupling ratios R_{12} and R_{13}, which are related to the ellipse fit amplitudes $\bar{A}_k$ and the reference light coupling ratios.

$$R_{12} = \frac{a_2}{a_1} \frac{\bar{A}_1}{\bar{A}_2} \qquad R_{13} = \frac{a_3}{a_1} \frac{\bar{A}_1}{\bar{A}_3}$$

The ratios a_2/a_1 and a_3/a_1 should typically be near unity, and in principle, can be determined experimentally.

In many circumstances, precise characterization of a_2/a_1 and a_3/a_1 may not be needed. If the measurement is AC coupled, the ratio $I_T(t)/I_R$ can be made relatively small (≤ 0.001) without sacrificing digitizer bandwidth. The dynamic baseline in the normalized signals would then be much smaller than the amplitude, unless there is a dramatic change in the target intensity or coherence. In the absence of additional characterization data, a reasonable approximation would be $R_{12} = R_{13} = 1$.

2.2.4 Two-phase measurements

When only two phases are recorded in a three-phase measurement, it is possible to synthesize the third phase under certain conditions. Assumptions about the target intensity variations or target/reference levels are required in the process, and these are assumptions may not be valid in all cases. In general, recording all three phases is strongly recommended.

To handle two-phase measurements, consider the normalized signals defined by Equation 2.10.

$$\tilde{D}_1(t) = \frac{1}{2}\sqrt{\frac{b_1}{a_1}}\frac{I_T(t) - \bar{I}_T}{\sqrt{I_R \bar{I}_T}} + \sqrt{\frac{I_C(t)}{\bar{I}_T}}\cos\Phi(t)$$

$$\tilde{D}_2(t) = \frac{1}{2}\sqrt{\frac{b_2}{a_2}}\frac{I_T(t) - \bar{I}_T}{\sqrt{I_R \bar{I}_T}} + \sqrt{\frac{I_C(t)}{\bar{I}_T}}\cos(\Phi(t) + \beta_+)$$

If the target intensity is relatively constant or $I_R \gg I_T$, the first term can be neglected. The signal ratio is then:

$$\frac{\tilde{D}_2(t)}{\tilde{D}_1(t)} = \frac{\cos\Phi(t)\cos\beta_+ - \sin\Phi(t)\sin\beta_+}{\cos\Phi(t)}$$

which leads to a simple quadrature reduction.

$$\tan\Phi(t) = \frac{D_y(t)}{D_x(t)}\frac{\cos\beta_+\tilde{D}_1(t) - \tilde{D}_2(t)}{\sin\beta_+\tilde{D}_1(t)} \tag{2.17}$$

Fringe shift is thus estimated from a two-phase measurement and used to synthesize the third signal; the baseline, amplitude, and phase shift of the third signal are the average of the two measured signals. A utility program called faker is included with the THRIVE program to perform this conversion.

2.3 Savitzky-Golay differentiation

Numerical differentiation is required to determine target velocity from the fringe shift measured by a displacement interferometer. Though conceptually straightforward, numerical differentiation amplifies high frequency information and can be problematic in the presence of noise. Smoothing can be used to reduce this effect, but doing so reduces the time resolution of a measurement. As a compromise, derivatives in THRIVE are calculated using the Savitszy-Golay method [13]; consistent smoothing is applied where appropriate.

Consider a signal s_k sampled on a uniformly spaced time grid t_k with spacing T.

$$t_k = t_r + (k - k_r)T$$

In the vicinity of t_r, the signal can be approximated as an polynomial of order M.

$$f(t) = \sum_{m=1}^{M+1} b_m \left(\frac{t - t_r}{T}\right)^{m-1} \rightarrow f(t_k) = \sum_{m=1}^{M+1} b_m (k - k_r)^{m-1}$$

The coefficients b_n $(n = 1..M+1)$ are determined by optimizing the residual χ^2 evaluated over N points about t_r.

$$\chi^2 = \sum_{k=1}^{N}\left(s_k - \sum_{m=1}^{M+1} b_m (k - k_r)^{m-1}\right)^2$$

$$\frac{\partial\chi^2}{\partial a_n} = -2\sum_{k=1}^{N}\left(y_k - \sum_{m=1}^{M+1} b_m (k - k_r)^{m-1}\right)(k - k_r)^{n-1} = 0$$

These equations form a linear system (scaled by N for precision considerations):

$$\sum_{k=1}^{N} \underbrace{\left[\left(\frac{k-k_r}{N}\right)^{n-1}\right]}_{L_{nk}} y_k = \sum_{m=1}^{M+1} \underbrace{\left[\sum_{k=1}^{N}\left(\frac{k-k_r}{N}\right)^{n+m-2}\right]}_{R_{nm}} \underbrace{\left(N^{m-1} b_m\right)}_{b'_m}$$

that can be solved via matrix division (*e.g.*, the MATLAB backslash operator).

$$b_m = \sum_{k=1}^{N} \underbrace{\left(\frac{1}{N^{m-1}}\ \tilde{R}\backslash\tilde{L}\right)_{mk}}_{w_{mk}} y_k \tag{2.18}$$

The best fit polynomial coefficients are the convolution of the signal with the weight matrix w_{mk}. Note that this matrix is independent of the signal, so the same weights can be used for all time locations.

The Savitzy-Golay weights can be used to smooth and differentiate a signal. To illustrate this point, consider the value of the smoothing function at the point t_r. Most of the terms in the summation of $f(t_r)$ are zero at this point with the exception of $m = 1$.

$$f(t_r) = b_1$$

The function derivative:

$$\frac{df(t)}{dt} = \sum_{m=2}^{M+1} \frac{(m-1)b_m}{T}\left(\frac{t-t_r}{T}\right)^{m-2}$$

has similar behavior at t_r, with $m = 2$ being the only non-zero term.

$$\frac{df(t_r)}{dt} = \frac{b_2}{T}$$

Continuing this logic leads to a general form the Savitzky-Golay derivative.

$$\frac{d^n(t_r)}{dt^n} = \frac{n!}{T^n}\ b_{n+1} \tag{2.19}$$

Calculating the n-derivative amounts to performing a convolution of the signal with $w_{n+1,k}$ and scaling the result by T^n.

Table 2.1 lists a few Savitzky-Golay weights of different orders for symmetric applications, where equal numbers of points are used on the left and right of the reference point. At low orders, the Savitzky-Golay method is identical to common forms of numerical smoothing and differentiation. For example, zero and first order smoothing is equivalent to local averaging; a three point, first order Savitzky-Golay derivative equivalent to the centered difference method [14]. Note that redundancies exist between adjacent orders—weights for five-point first and second order smoothing are precisely the same, as are the five-point derivative weights for those orders. This repetition stems from the structure of the R_{ki} matrix, which is zero whenever $i + k$ equals an odd number.

The choice of order and number of points in the Savitzky-Golay method is driven by several factors. The order must be compatible with the derivative of interest and a sufficient number of

Table 2.1. Selected list of symmetric Savitzky-Golay weights for order M and number of points N. The $(M+1)\times N$ weight matrix is calculated from Equation 2.18; each table entry is the $n+1$ row of this matrix, where n is the derivative level.

M	N									
					Smoothing weights					
0	3				0.3333	0.3333	0.3333			
0	5			0.2000	0.2000	0.2000	0.2000	0.2000		
1	3				0.3333	0.3333	0.3333			
1	5			0.2000	0.2000	0.2000	0.2000	0.2000		
2	5			-0.0857	0.3429	0.4857	0.3429	-0.0857		
2	7		-0.0952	0.1429	0.2857	0.3333	0.2857	0.1429	-0.0952	
2	9	-0.0909	0.0606	0.1688	0.2338	0.2554	0.2338	0.1688	0.0606	-0.0909
4	7		0.0216	-0.1299	0.3247	0.5671	0.3247	-0.1299	0.0216	
4	9	0.0350	-0.1282	0.0699	0.3147	0.4172	0.3147	0.0699	-0.1282	0.0350
					First derivative weights					
1	3				-0.5000	0.0000	0.5000			
1	5			-0.2000	-0.1000	0.0000	0.1000	0.2000		
2	5			-0.2000	-0.1000	0.0000	0.1000	0.2000		
2	7		-0.1071	-0.0714	-0.0357	0.0000	0.0357	0.0714	0.1071	
2	9	-0.0667	-0.0500	-0.0333	-0.0167	0.0000	0.0167	0.0333	0.0500	0.0667
4	7		0.0873	-0.2659	-0.2302	0.0000	0.2302	0.2659	-0.0873	
4	9	0.0724	-0.1195	-0.1625	-0.1061	0.0000	0.1061	0.1625	0.1195	-0.0724

points must be used to support that order. For the n-th derivative, the order must be at least $n+1$, which requires no less than $n+2$ points. By using more points, greater smoothing can be achieved, possibly at the expense of resolving rapid signal features.

CHAPTER 3

Program overview

This chapter presents an overview of the THRIVE program. First, program installation and execution instructions are given. Next, the analysis stages used by the program are defined. Finally, general characteristics of the graphical interface are disucussed.

3.1 Installing and running THRIVE

THRIVE exists in two formats: a MATLAB version and a Windows executable version. The former runs within MATLAB, while the executable version may be used on Windows systems without MATLAB. Installation of each version is considerably different and will be described separately. Figure 3.1 illustrates the files contained in THRIVE version 1.0. These files should be copied to a local directory before installation.

3.1.1 MATLAB version

The MATLAB version of THRIVE is intended for release 2007A or later. Earlier versions (perhaps as far back as 7.0) may also work but are not supported. A valid MATLAB license (`http://www.mathworks.com`) is required.

To install the program, add the `matlab` directory to the MATLAB path, using either the "addpath" command or the "Set path" tool on the "File" menu. Only the main folder itself, not the private subdirectory, should be added to the path.

After installation is complete, the program can be started by typing "THRIVE" at the command line. While running, the program is independent from the main workspace. As such, program variables will not overwrite existing memory, and graphics created by MATLAB will not be rendered in the THRIVE window.

3.1.2 Windows executable

The executable version of THRIVE is intended for Windows XP. The program may operate in older versions of Windows but is not supported. The executable version of THRIVE has not been tested on Windows Vista but should presumably work.

- `matlab` directory
  - THRIVE.p
  - faker.p
  - `private` subdirectory
- `winexe` directory
  - `MCRInstaller2007a.exe`
  - `THRIVE.exe` and `THRIVE.ctf`
  - `faker.exe` and `faker.ctf`
- `bench` directory
  - `benchA_1.txt` through `benchA_5.txt`
  - `benchB_1.txt` through `benchA_4.txt`
  - `benchC_1.txt` through `benchA_4.txt`

Figure 3.1. File structure for THRIVE version 1.0

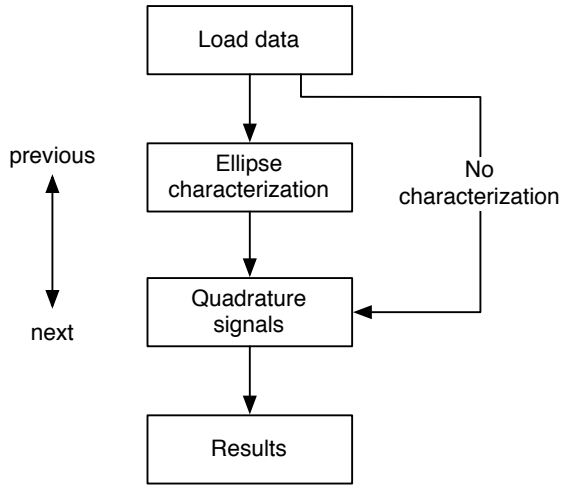

Figure 3.2. Analysis overview

After the contents of the `winexe` directory have been copied to a local directory, double click the `MCRInstaller2007a.exe` program and accept all default choices in the installation. This process installs necessary libraries and support functions for THRIVE, and needs to be performed *once* for each machine (desktop, laptop, etc.) where the program is to be used.

When the MCR installer is complete, THRIVE can be launched by double clicking on `THRIVE.exe`. Initial launch of the program will be somewhat sluggish as various routines are unpacked for the first time; subsequent launches should be considerably faster.

3.2 Analysis overview

Figure 3.2 illustrates the analysis stages of the THRIVE program. First, data is loaded into the program from either a single file or three separate files. Next, the data undergoes ellipse characterization to determine various parameters needed in the analysis. Using these parameters, the data signals are reduced to a pair of quadrature signals, from which various results (fringe shift, position, and velocity) are calculated. A summary of each stage is given below.

3.2.1 Loading data

The program begins with "Load data" screen. Within this screen the user can select data file(s), specify time ranges, and select the type of characterization used in the analysis. When these operations are complete, the users presses the "Next" button to continue.

THRIVE accepts three-phase[1] signal data stored either as a single data file or separate data files. Single file mode accepts text files with an arbitrary length/format text header following by four numerical columns (delimited by white space or commas). The first column in a single text file is assumed to be time, the second column D_1, and the remaining columns D_2 and D_3; the order of the last two columns can be specified within the graphical interface. Separate file mode accepts individual text files for each data signal. All three files should have two numerical columns (time and signal), and can have an arbitrary text header.

No explicit file size limits are built into the THRIVE program. The maximum number of data points is limited only by the operating system and the user's patience. For 32-bit operating systems, 1-2 million sample points is acceptable, though somewhat sluggish; ten million or more will cause the program to exceed 32-bit memory limitations. THRIVE has not yet been tested on a 64-bit platform, but presumably much larger data sets could be loaded. For optimal performance, data should be cropped to regions of interest before being loaded into THRIVE, and the experiment time (defined below) reduced as much as possible.

Once data is loaded into the program, the user may select several time ranges for the analysis. "Characterization time" is intended for durations where the signals are exposed to constant light conditions; data within this range is fed into subsequent characterization stages. "Experiment time" defines the period where analysis is to be performed; data outside this domain is not processed. The boundaries of each region may be entered manually or selected with the mouse. To specify

[1] Two-phase measurements can be converted to a three-phase format using a utility (faker) included with the THRIVE package. Section 2.2.4 describes the synthesis of the third signal.

boundaries that include the beginning or end of the data set, enter -inf or +inf ($\pm\infty$).

The final option set by the "Load data" screen is the characterization mode. The default choice is "Ellipse fit", which allows the program to compensate for non-ideal measurements. Ellipse characterization can be skipped by selecting "None", which tells the program to assume that the measurement was made with an ideal system. Users are strongly encouraged to use the default option.

3.2.2 Ellipse characterization

If "Ellipse fit" characterization is selected, users are guided to the "Ellipse characterization" screen. Within this screen the user controls ellipse fits of the $D_1 - D_2$ and $D_1 - D_3$ signal pairs. If necessary, the user can return to the "Load data" screen by pressing the "Previous" button. When the characterization is complete, the user can continue the analysis by pressing the "Next" button.

The two ellipse fits are controlled by eight numerical parameters: three baseline values, three amplitudes, and two phase shifts. Parameters may be entered manually or determined by least squares optimization. "Optimize parameters" performs this operation, allowing individual parameters to remain fixed as dictated by the users. The "Guess parameters" button launches a direct (non-iterative) ellipse fit procedure [15]. This fit determines all eight parameters, resetting all fixed quantities. The guess feature is intended to provide a quick set of reasonable parameters for a nearly complete characterization ellipse, while the optimize feature is meant for refining parameters based on additional information and/or intuition.

After the ellipse fits are complete, the user may choose how the program interprets the parameters. By default, THRIVE assumes that the measurements are DC coupled and that each detector receives most of its light from the reference source rather than the target. These assumptions dictate how the program calculates the scaling ratios R_{12} and R_{13}. To change this interpretation, users can change the popup menus to reflect the true lighting conditions; if the reference light exactly matches the target light level, both choices will yield the same result. The assumption decisions can be made individually or linked together, giving the user two or eight possible choices. For AC coupled measurements, assumptions about reference and target light levels are disabled, and users can enter R_{12} and R_{13} values manually.

3.2.3 Quadrature reduction

The "Quadrature signals" screen shows the results of quadrature reduction using either ellipse characterization or ideal analysis, depending on the user's selection on the "Load data" screen. This screen only shows the reduced quadrature signals in various forms—there are no adjustable parameters. The user can return to "Ellipse characterization" or "Load Data" by pressing the "Previous" button or continue onto the results by pressing the "Next" button.

Four parameters, determined by fitting the reduced quadrature signals (in the characterization domain) with an ellipse, are shown in this screen to indicate how well the quadrature signals match a circle centered at the origin. Ideally, the horizontal and vertical centering error should be at 0%, the aspect ratio at 100%, and the quadrature error at 0°. Substantial deviations from these values should alert the user to measurement imperfections that require ellipse characterization (if

no characterization was selected) or revisions to the ellipse fit.

Quadrature signals can be displayed two ways on this screen. First, the $D_x - D_y$ signals can be plotted as an ellipse, using data either from the characterization or experiment time range. The characterization ellipse is shown as a heavy solid line to provide a visual sense of how well quadrature reduction operates on the data. The quadrature signals may also be displayed as a function of time.

3.2.4 Results

The "Results" screen is the last stage of the THRIVE program, where users may view the calculated fringe shift, position, or velocity. Final analysis parameters are set in this screen, and data can be exported from the program to a text file. Users can step back to the "Quadrature signals" screen by pressing the "Previous" button.

A key setting in the "Results" screen is the interferometer type (displacement or velocity), which determines how THRIVE interprets fringe shift. Displacement configuration is the default selection.

The three basic parameters in this screen are the fringe constant, the fit order, and the number of fit points. The fringe constant determines how changes in fringe shift correspond to position or velocity (depending on interferometer type), and is set by default to 775×10^{-7} (half of a 1550 nm wavelength). The remaining two parameters define the order and number of points used in a Savitzky-Golay smoothing algorithm. Parameters are not applied until the user presses the "Update Plot" button, and invalid parameter entries (*e.g.*, non-integer Savitzky-Golay parameters) are corrected at that time. The Savitzky-Golay window size is updated with the plot to show users the time range over which smoothing occurs. Boundary points on each side of the data within half of this time range are removed from the output.

Data are exported from THRIVE using the "Export" button. The file name for export can be entered manually or chosen interactively via the "select" button. Note that once an export name has been entered into the edit box, pressing the export button immediately overwrites that file—no overwrite warnings are given.

3.3 The graphical interface

This section highlights graphical features common to all portions of the THRIVE program.

3.3.1 Menu items

Each screen in the THRIVE program has "Program" menu and a "Help" menu. The program menu allows the user to restart and exit the program. Restart closes and relaunches the program, clearing all entries and returning the program to its default state. The help menu provides general information about THRIVE and briefly summarizes the operations that can be performed in the current screen.

3.3.2 The toolbar

Each screen in THRIVE contains a toolbar with the following operations:

1. Set working directory
   Interactively select the current directory
2. Zoom
   Enables zoom mode. Plots can be zoomed into with either a left mouse click or click and drag. Shift-click zooms out and double click restores the original view. Press the right mouse button (or control-click) for additional options.
3. Pan
   Enables pan mode, where user can drag though various parts of a plot.
4. Auto scale
   Automatically scale the x- and y-limits of a plot on the data it contains. If only one plot is present, it is immediately scaled. When multiple plots are present, the user can click on specific plots to scale (shift-click scales all plots).
5. Tight scale
   Tightly scale the x- and y-limits of a plot based on the data it contains.
6. Manual scale
   Manually scale the x- and y-limits of a plot.
7. Data cursor
   Display (x, y) data of points on a line. Press the right mouse button (or control-click) for additional options.
8. ROI statistics
   Allows the user to drag a rectangular region of interest (ROI). Statistical quantities (mean, deviation) for all data inside that ROI are displayed in a separate window.
9. Help
   Displays a summary of toolbar operations.

Toolbar settings are screen specific, so each screen can exist in a different mode.

Toolbar operations are disabled during time range selection, and are re-enabled when time range selection is complete. If a toolbar operation is activated during time range selection, it must be de-activated before that time range selection can proceed.

3.3.3 Cloning plots

Every plot in THRIVE contains a "clone" button in the upper right hand corner. Pressing this button copies the plot to a separate figure window. An arbitrary number of plot clones may exist at any given time. Cloned figures are time-stamped for identification purposes, and can be saved

to a file using the "File" menu or the "Save figure" button (disk icon). The default format is a MATLAB figure, but various graphical formats (*.pdf, *.jpg, etc.) may also be selected.

A key application of plot cloning is to allow users to see data from a preceding analysis stage. For example, the raw signal plot may be cloned from the "Load data" screen and kept open while the user moves onto later screens. The intent of this feature is to help users understand and interpret measurements by simultaneously viewing different stages of the analysis. Note that cloned plots remain static after creation, and are not updated by the main program.

CHAPTER 4
Using THRIVE

This chapter describes the practical use of the THRIVE program. First, a few platform specific details are provided. Next, a complete analysis example is presented. Finally, solutions to common analysis problems are presented.

4.1 Platform notes

THRIVE was designed in OS X, but has been formatted to work on Windows and Linux platforms. Apart from differences in how various controls (*e.g.* popup menus) are rendered, the graphical interface is similar on all platforms. Known differences are described below.

Window resizing on systems using X11 (such as Linux and OS X) can be a problem if the figure becomes smaller than the minimum size allowed by the program. When this happens, the figure is forced back to its minimum without refreshing, which may hide some graphics objects. Resizing the figure just slightly above its minimum limits corrects this problem.

File names specified in THRIVE must adhere to the local operating system conventions. For example, a file "file.txt" in a subdirectory "data" would be specified as `./data/file.txt` in Unix/OS X and `.\data\file.txt` in Windows. Files selected interactively with the "select" button automatically use the local naming convention.

4.2 Analysis example

Figure 4.1 show benchmark data set A-4 loaded into THRIVE. The data is contained in a single file, `benchA_4.txt`, located within the bench subdirectory. This data represents a non-ideal measurement, obtained with an imperfect displacement interferometer and variable light conditions (full details are given in the the next chapter). Signal noise and digitizer limitations have also been added to simulate a real measurement. The characterization time for this measurement has been specified as $-80 \times 10^{-9} \leq t \leq 800 \times 10^{-9}$, a region that appears to have relatively constant signal amplitude. The experiment time range has been left at the default value so that entire data record will be analyzed.

The characterization ellipses for this example are shown in Figure 4.2. Since the characterization

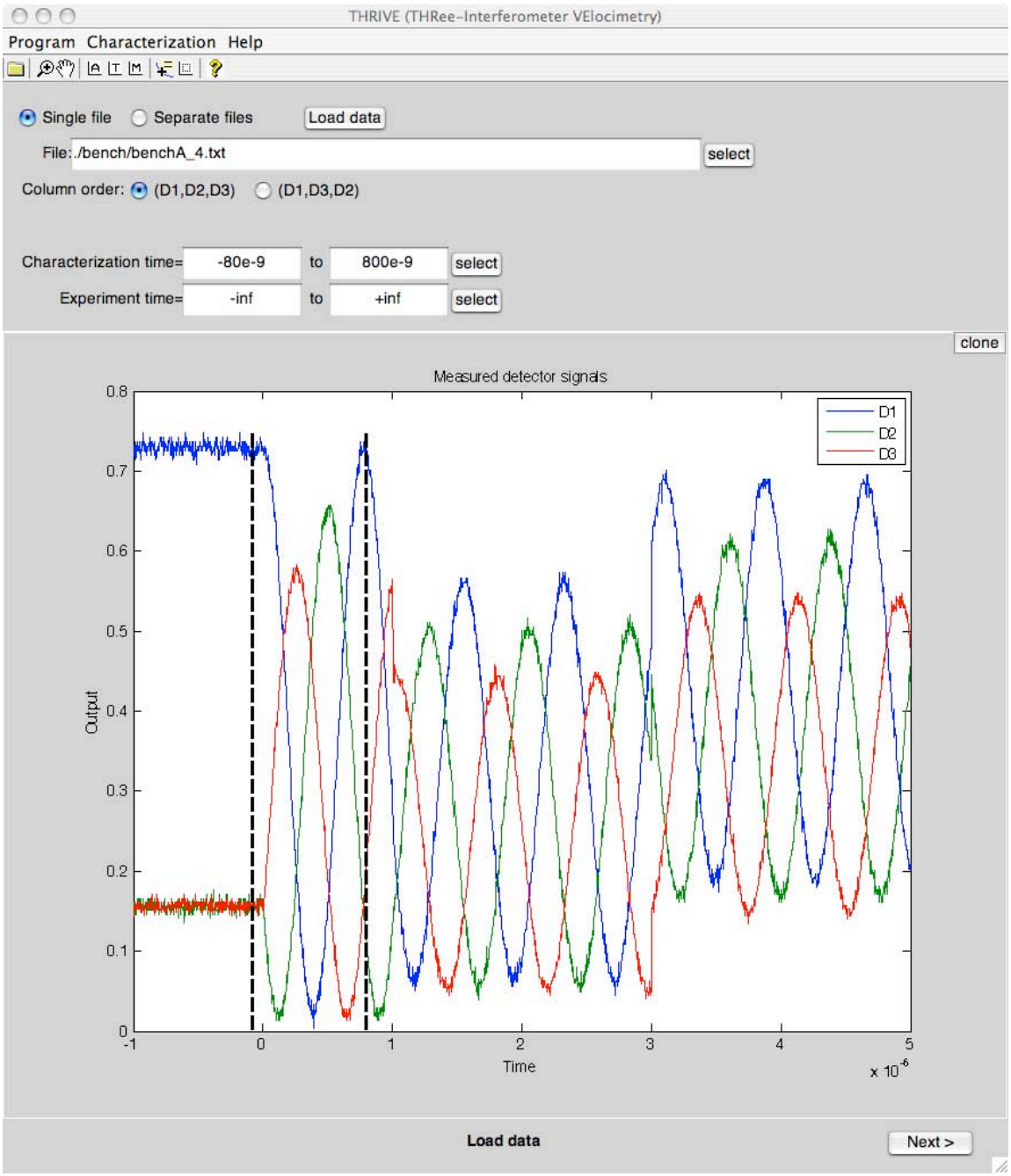

Figure 4.1. Load data example

data completely spans the ellipse, the parameter guess function finds an adequate solution. Optimization produces slightly different parameters, but the final results are not substantially different. The phase shifts determined by the fit (124.7° and 119.7°) are quite similar to the values specified in the benchmark problem (125° and 120°).

Figure 4.3 shows the reduced quadrature signals plotted as an ellipse. Remarkably, the ellipse is very near its ideal state: centering is within 0.1%, the aspect ratio within 0.4%, and quadrature error is less than 0.1°. By comparison, if one omitted ellipse characterization, the quadrature signal centering would be off by nearly 10%, the aspect ratio by 20%, and the quadrature error would be nearly 6°. This sort of imperfection would lead to noticeable variations in the final velocity result.

Figures 4.4–4.5 show the position and velocity results for this example. The position results are relatively smooth, while the velocity is quite noisy, even when first order smoothing is applied over 21 data points. Smoother steady state performance can be obtained by increasing the number of smoothing points, though this benefit comes with the loss of time resolution, particularly noticeable at the steep velocity rise. The actual velocity history in this example is an instantaneous velocity step, from 0 to 1 m/s, at time $t = 0$, which is consistent with the average behavior in Figure 4.5.

4.3 Analysis hints

Common analysis questions about THRIVE include direction control, ellipse characterization, and the choice of smoothing parameters. Suggestions and hints on each of these topics is given below.

4.3.1 Direction control

It is not uncommon to obtain negative velocities in THRIVE. Negative velocities for motion toward the observer (assumed here to be positive velocity) results from an inconsistent data ordering. The problem can be dealt with in two ways: exchanging the D_2 and D_3 signals or inverting the fringe constant sign. The latter method is more convenient as it can be done immediately when negative velocity is observed; the former method requires the user to return to the "Load data" screen.

4.3.2 Ellipse characterization

Selecting a useful characterization range is important to the operation of the THRIVE program. If the data signals vary substantially in amplitude, it is important that the time range be sufficiently narrowed to extract a single ellipse. Characterization ranges that contain variable light conditions will lead to an imperfect ellipse fit. The characterization range need not be any wider than a single fringe. It is important, however, that the range cover 25% or more of a fringe; otherwise, the ellipse fit and quadrature characterization stages may run into numerical problems. Parameter fixing can be a very useful approach in ellipse characterization of a partial fringe. Alternately fixing center parameters (such as phase shift) while optimizing other (such as ellipse amplitude) can also help ellipse characterization of partial fringe data.

When the interferometer signals become highly complicated, it may be advisable to perform

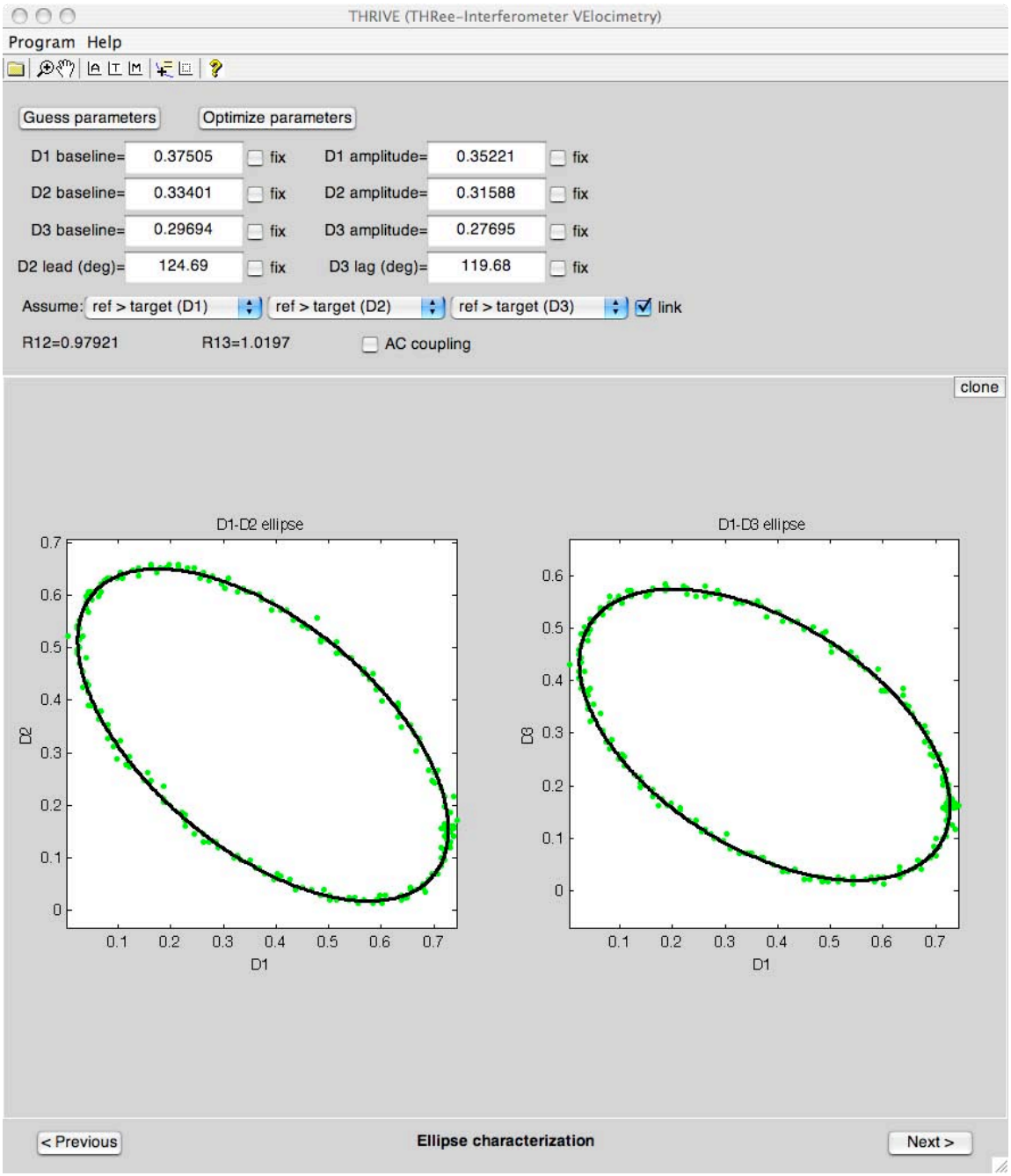

Figure 4.2. Ellipse characterization example

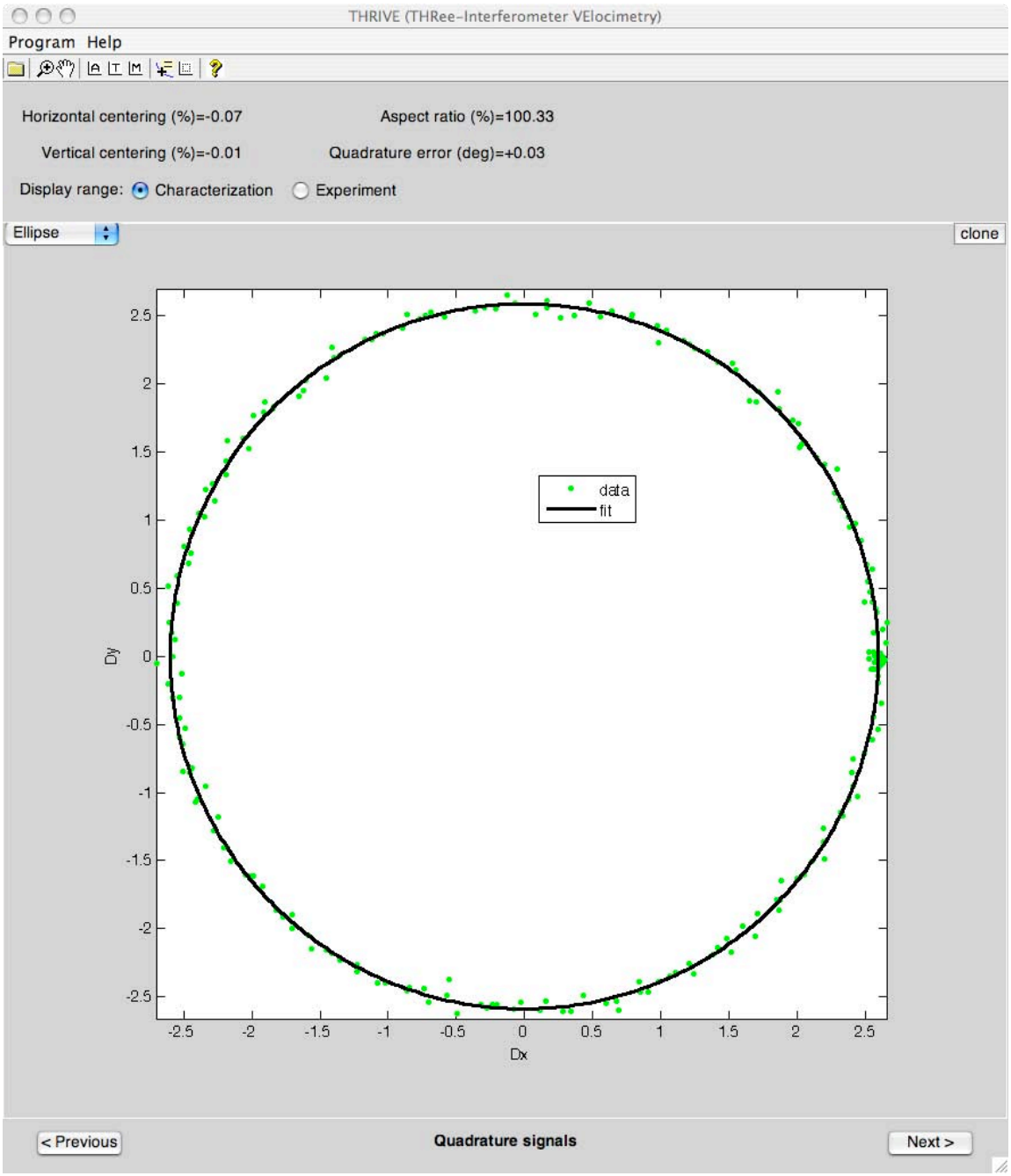

Figure 4.3. Quadrature signals example

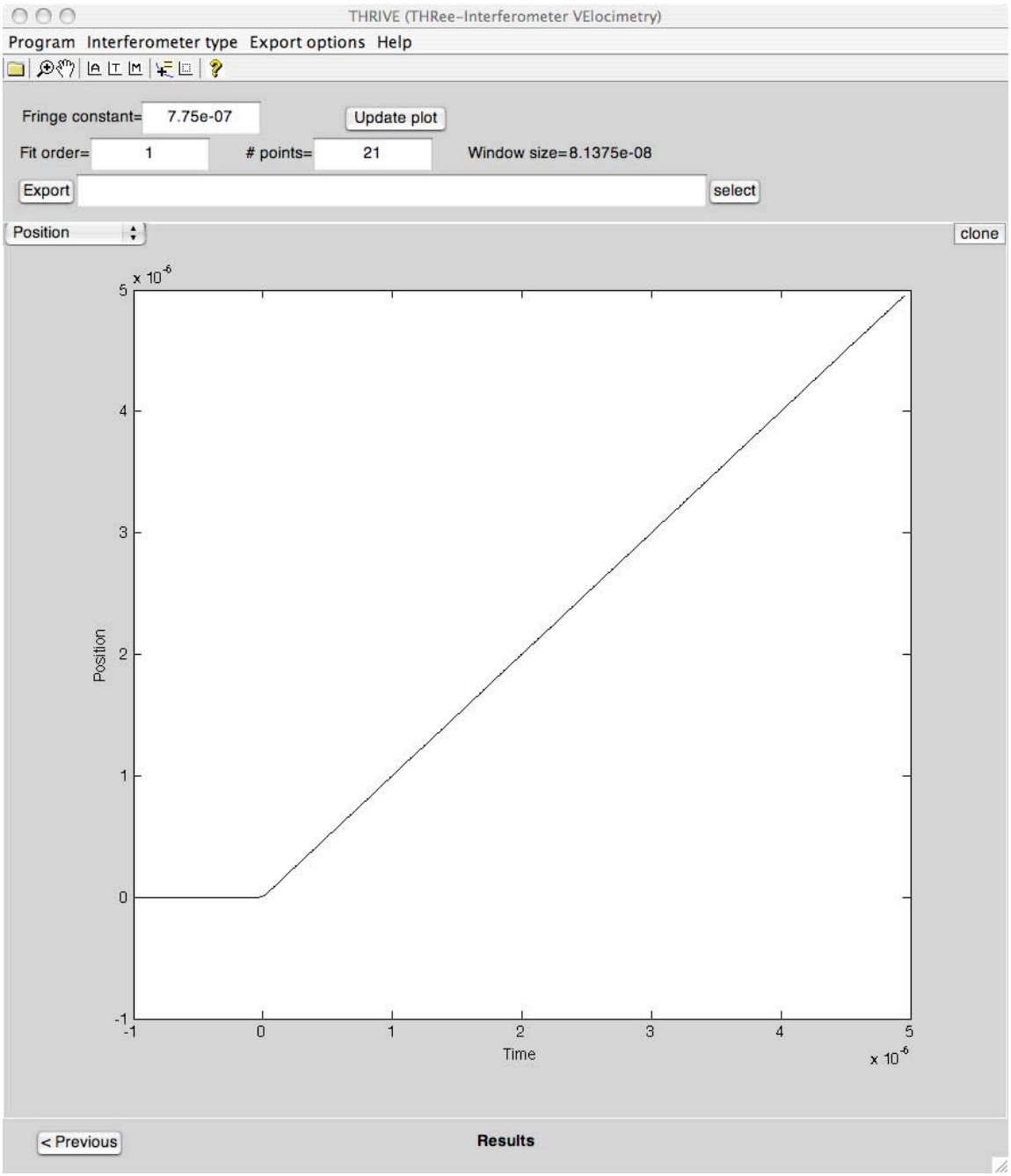

Figure 4.4. Position results example

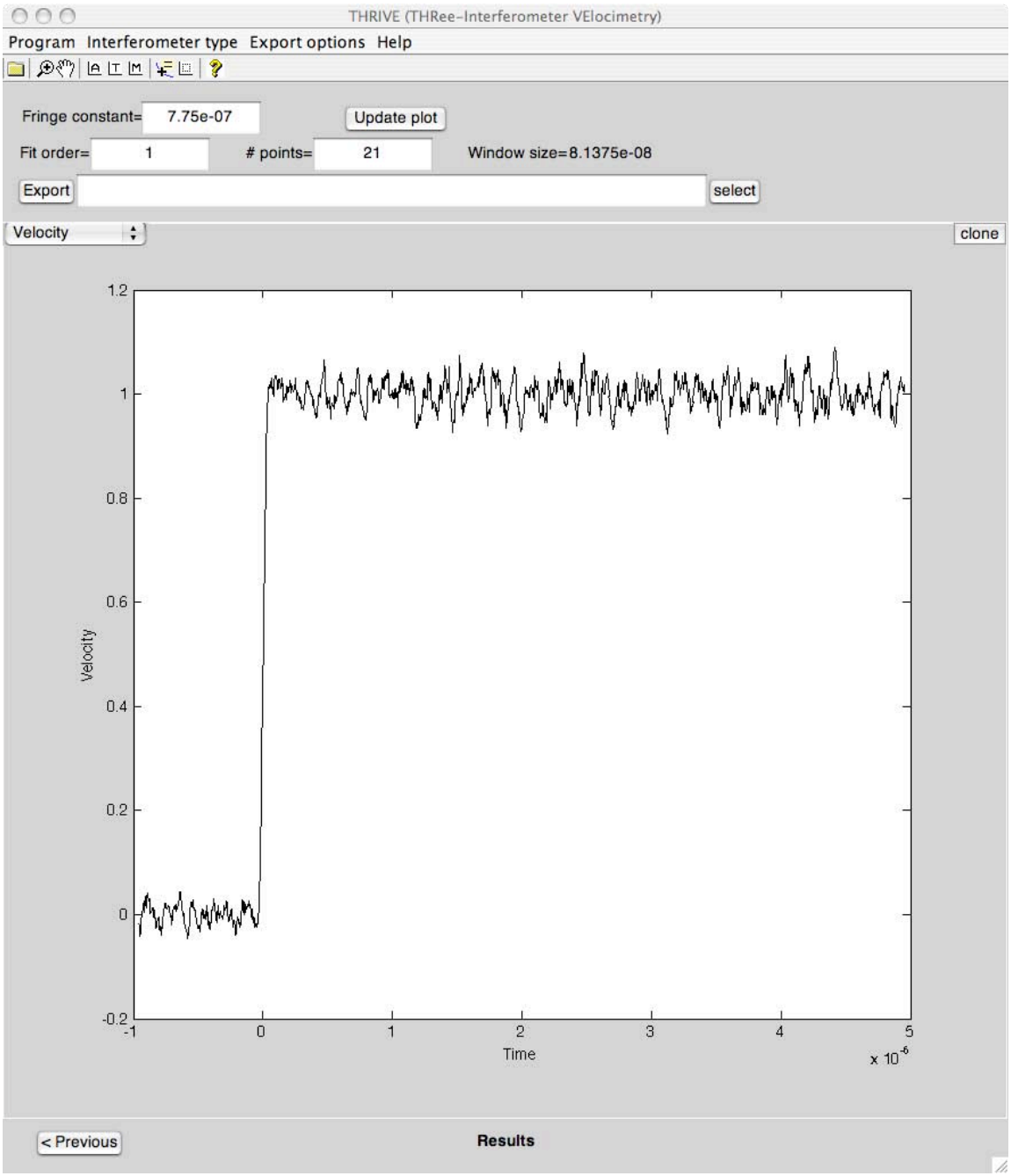

Figure 4.5. Velocity results example

ellipse characterization on set of reference signals rather than the actual measurement. For example, signals are often acquired prior to a single-event measurement via "tap tests". Such data can be used in THRIVE to determine phase shifts (at the very least). Once complete, the user can step back to the load screen, read in the measurement of interest, and return the ellipse characterization screen. Ellipse parameters from the reference data will still be present and can be used in constrained optimization.

4.3.3 Smoothing parameters

Smoothing parameter selection is based on the competing desire to reduce noise effects and preserve time resolution. Large fit orders retain high frequency information, while large smoothing regions attenuate high frequency transients. The precise choice will depend upon the level of signal noise, the sampling rate, and the relevant features of interest.

The fit order describes the polynomial allowed to pass through the points in each smoothing region. By selecting this order, the user controls the highest derivative allowed within each region. For example, setting the fit order to 1 in a displacement interferometer measurement forces linear displacement and constant velocity in each region. A useful rule of thumb is to select a fairly low fit order (2–4) and decide the time range over the which the relevant derivative could be neglected. If the time range is wider than a particular feature of interest, however, the fit order must be increased to avoid bias effects [16].

CHAPTER 5

Benchmark problems

Several benchmark problems are included with THRIVE to give users experience with the program. The data files for each benchmark problem are located within the `bench` directory and span three distinct velocity histories (A–C). Several variations of each history are presented to illustrate different analysis concepts. First, a velocity step is analyzed for different measurement conditions. Similar analysis of a velocity ramp and velocity pulse are also provided.

A maximum velocity of 1 m/s is prescribed in each benchmark problem, and the signals represent measurements from a displacement interferometer (PDV) operating at 1550 nm. Problems containing an intrinsic time scale are expressed as a function of the minimum beat period ($T = 775$ ns in this case). With the appropriate time scaling, the results can be applied to higher or lower velocities.

5.1 Velocity step

Benchmark problems A-1 to A-5 are based on an instantaneous velocity step at time $t = 0$.

$$v(t) = \begin{cases} 0 & t < 0 \\ v_m & t \geq 0 \end{cases} \tag{5.1}$$

Benchmark A-1 (`benchA_1.txt`) contains synthetic PDV signals for this velocity history under ideal conditions. Ideal conditions in this setting mean that: the 3×3 coupler divides all inputs equally and yields perfect 120° phase shifts; all detectors (DC coupled) have precisely the same sensitivity and coupling efficiency; light from the moving target is constant, completely coherent, and precisely matched to the reference; the measured signals are noise-free and sampled by a perfect 32-bit digitizer. These conditions are never met (certainly not simultaneously) in practice, so this data serves as the best case scenario. The signals in this data set are over-sampled by 100× the Nyquist limit, meaning that there are 200 samples/cycle.

5.1.1 Noise-free signals

Benchmark A-2 (`benchA_2.txt`) relaxes the constraints of the ideal case. In this problem: the second signal leads the first by 125° (rather than 120°); the 3×3 coupler output to the second and thirds signals varies by 2 and 4% (respectively) from the first signal; the second and

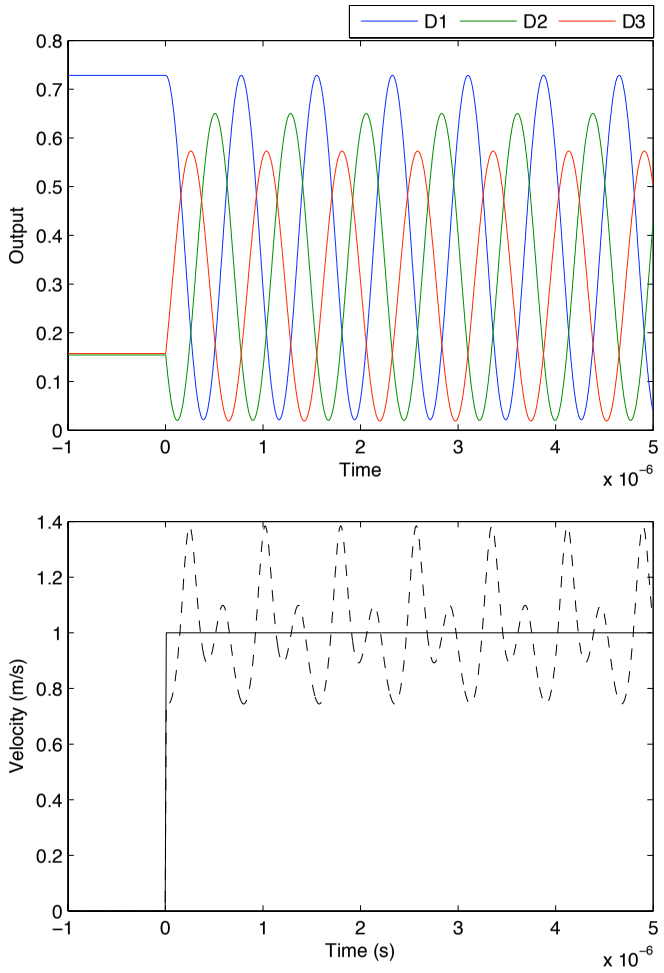

Figure 5.1. Imperfect measurement of a velocity step (benchmark problem A-2)

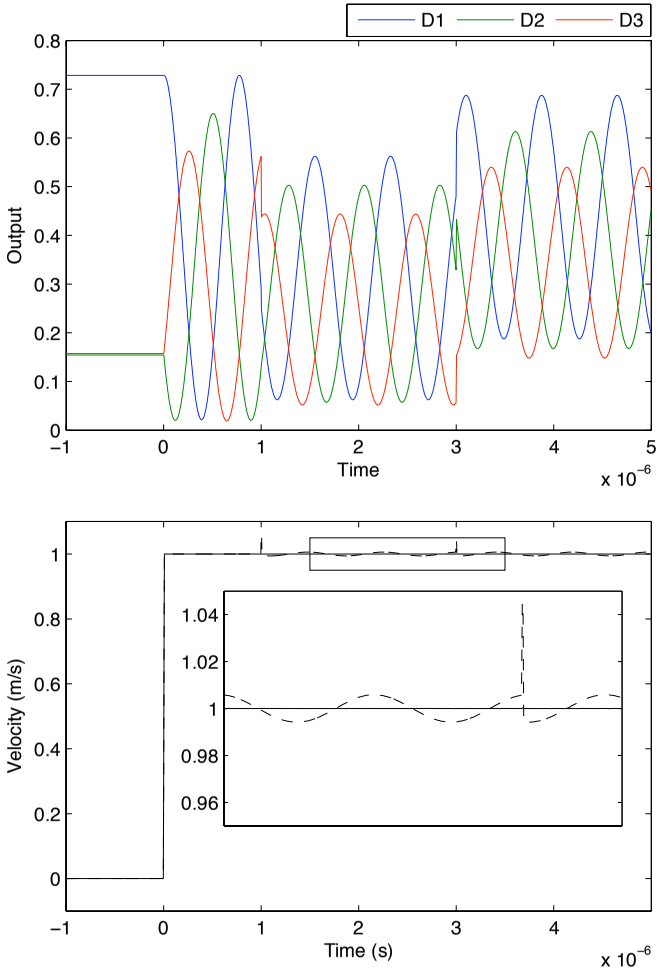

Figure 5.2. Imperfect measurement of a velocity step under variable light conditions (benchmark problem A-3)

third detectors are 10% and 20% less sensitive (respectively) than the first detector; coherent light from the target is only 50% that of the reference level. Figure 5.1 shows the signals produced by this imperfect measurement, along with two different analysis results. The dashed line indicates the velocity calculated without regard to the system imperfections. The solid line shows a more refined approach, using ellipse characterization to properly shift and scale the detector signals. The oscillations in the first velocity result from imperfect quadrature reduction. As a result, the quadrature signals are not exactly 90° out of phase, are not precisely centered at the origin, and have slightly different amplitudes. Ellipse characterization avoids these problems and yields the correct velocity history.

Benchmark A-3 (`benchA_3.txt`) uses the same imperfections as A-2 and introduces target light variations, both in magnitude and coherence. Figure 5.1 shows a variation of the previous example where coherent light intensity drops by 50% some time after the onset of motion, followed by incoherent emission at a later time. The two results shown in this case both utilize ellipse characterization. The difference between these two curves stems from the ellipse parameter interpretation. The solid curve assumes that the detectors receive most their light from the reference input (correct in this case), while the dashed line assumes more light comes from the target. The wrong assumption leads to velocity jumps at the transition between different regions of the signal (about 4.5%) and steady state oscillations (about 0.5%) between these regions. These effects occur in situations of changing light intensity and scale with the magnitude of the intensity modulation.

5.1.2 Noisy signals

Benchmark A-4 (`benchA_4.txt`) is the same as A-3 with the addition of 1% signal noise and discrete sampling by a 7-bit digitizer. Seven bit digitization is chosen to be representative of a real measurement. Most fast digitizers (> 1 GHz) are limited to eight bits, and some head space is typically needed to prevent signals from going off-scale. The inset in Figure 5.3 shows the velocity result with the default data smoothing (three points), while the main curve shows linear smoothing over 51 points.

Benchmark A-5 (`benchA_5.txt`) is a similar to A-4, but the oversampling has been reduced from 100× to 10×. Figure 5.4 shows the velocity result (five point smoothing).

5.2 Velocity ramp

Benchmarks B-1 to B-4 are based on a linear velocity ramp over a rise time τ.

$$v(t) = \begin{cases} 0 & t < 0 \\ v_m\,(t/\tau) & t \geq 0 < \tau \\ v_m & t \geq 0 < \tau \end{cases} \tag{5.2}$$

Two rise times, one slower than the beat period and one equal to the beat period, are considered.

5.2.1 Slow rise time

Benchmark B-1 (`benchB_1.txt`) contains the ideal PDV signals for a slow velocity ramp, where $\tau = 5T$. Benchmark B-2 (`benchB_2.txt`) uses the system imperfections from benchmark A-2

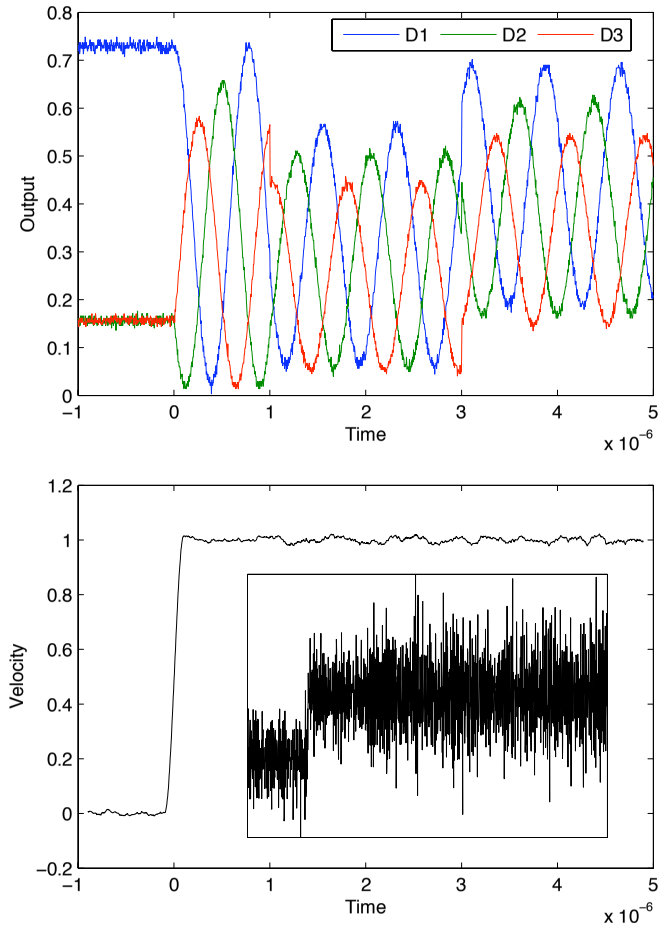

Figure 5.3. Imperfect measurement of a velocity step with variable light conditions and noise/digitizer limitations (benchmark problem A-4)

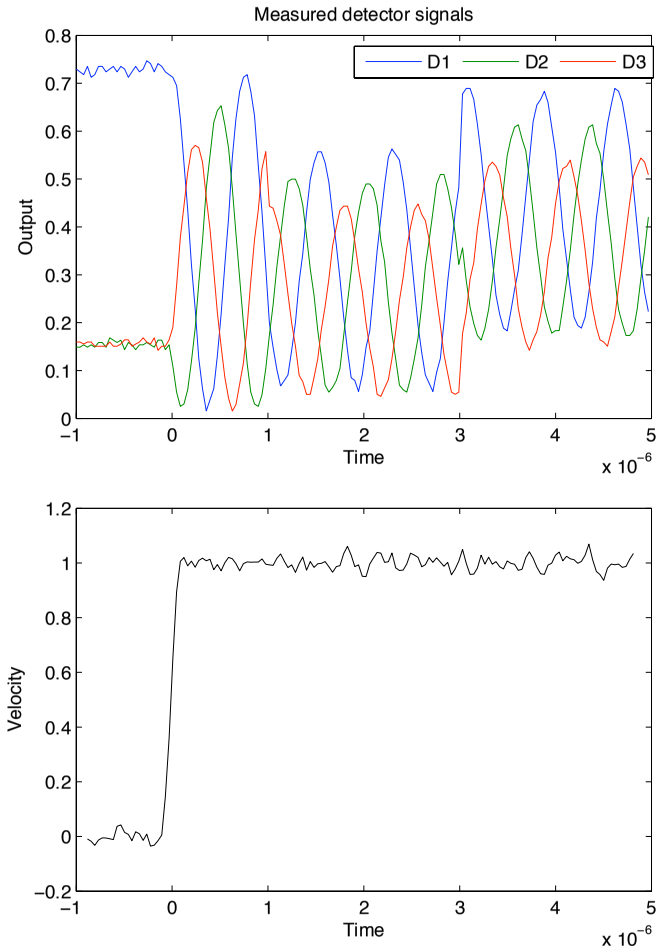

Figure 5.4. Imperfect measurement (with reduced oversampling) of a velocity step with variable light conditions and noise/digitizer limitations (benchmark problem A-5)

(imperfect phase shifts and coupling, variable detector sensitivity, unmatched target/reference light levels) on the same linear velocity ramp. Figure 5.5 shows the signals for benchmark B-2 and the calculated velocity history. The red dashed curve in the lower plot indicates the true velocity history, while the solid black line shows the noisy result after first order smoothing over 51 data points.

5.2.2 Fast rise time

Benchmark B-3 (`benchB_3.txt`) contains ideal PDV signals for a fast velocity ramp $\tau = T/5$; benchmark B-4 (`benchB_4.txt`) is the same problem with the system imperfections described in benchmark A-2. Figure 5.6 shows the signals for benchmark B-4 and the calculated velocity history. Only a portion of the velocity history, indicated by the vertical lines of the upper plot, is displayed to highlight the transient period. The red dashed curve in the lower plot indicates the true velocity history, while the solid black link shows the noisy result after first order smoothing over 51 data points. Unlike the slower rise problem, there is a noticeable difference between the two curves, particularly at the onset and completion of the ramp.

5.3 Velocity pulse

Benchmark problems C-1 to C-4 are based on a Gaussian velocity pulse.

$$v = v_m \exp\left[-\frac{-(t-t_0)^2}{2(\tau/6)^2}\right] \tag{5.3}$$

The width of this pulse is tailored so that the vast majority of the motion is contained within time τ. Unlike the previous examples, the signals are AC coupled. Two different pulse times scales are considered.

5.3.1 Slow pulse

Benchmark C-1 contains ideal PDV signals for a slow velocity pulse ($\tau = 5T$). Benchmark C-2 is based on the same velocity history, adding the system imperfections described in benchmark A-2. Figure 5.7 shows the signals for benchmark C-2 and the calculated velocity history. The red dashed curve in the lower plot indicates the true velocity history, while the solid black link shows the noisy result after first order smoothing over 51 data points.

5.3.2 Fast pulse

Benchmarks C-3 and C-4 are similar to C-1 and C-2 with change to a fast pulse width ($\tau = T/5$). Figure 5.8 shows the signals for benchmark C-4 and several different velocity calculations. The red dashed line is the correct velocity history, while the black dash-dot line is the noisy result smoothed over 51 points with a first order method. The peak velocity of the latter substantially undershoots the correct result, and the pulse is considerably wider. This effect is a result of a low order bias, which can be removed by increasing the fit order to six (solid black curve). In doing so, the calculated velocity more closely matches the true velocity, although new features (negative velocities) are added in the process.

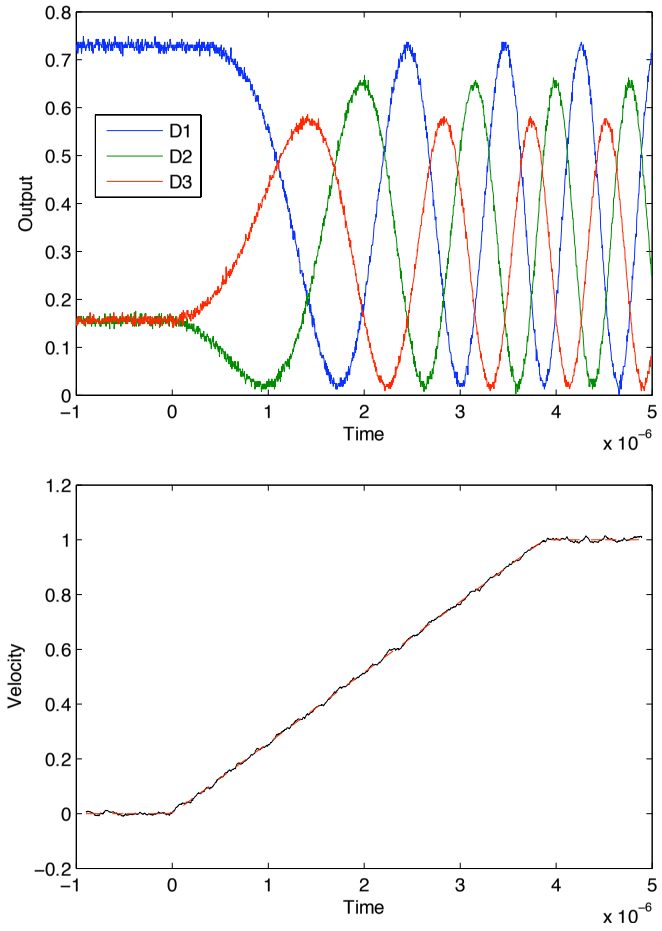

Figure 5.5. Imperfect measurement of a slow velocity ramp (benchmark problem B-2)

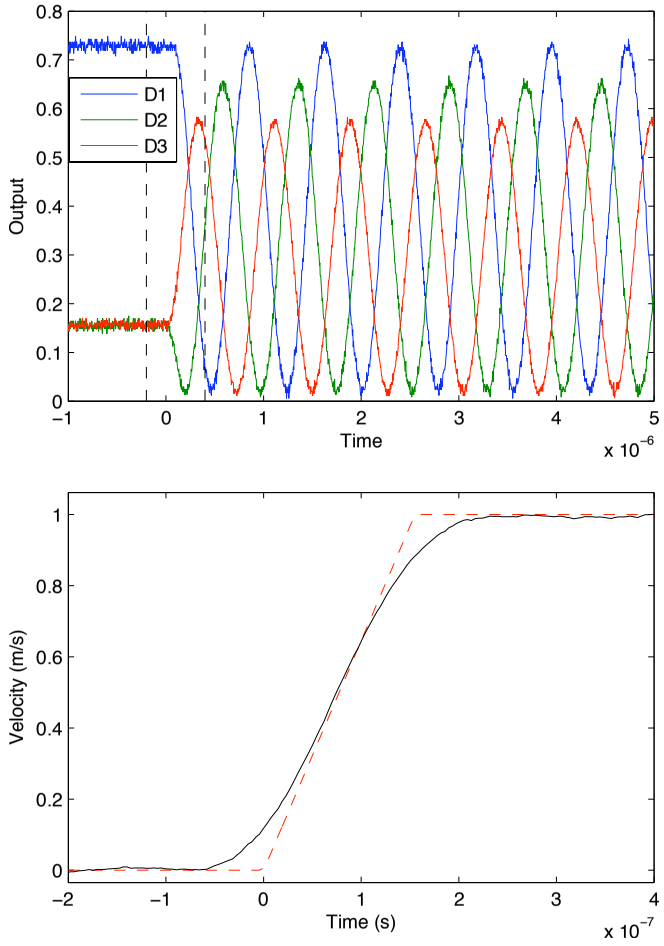

Figure 5.6. Imperfect measurement of a fast velocity ramp (benchmark problem B-4)

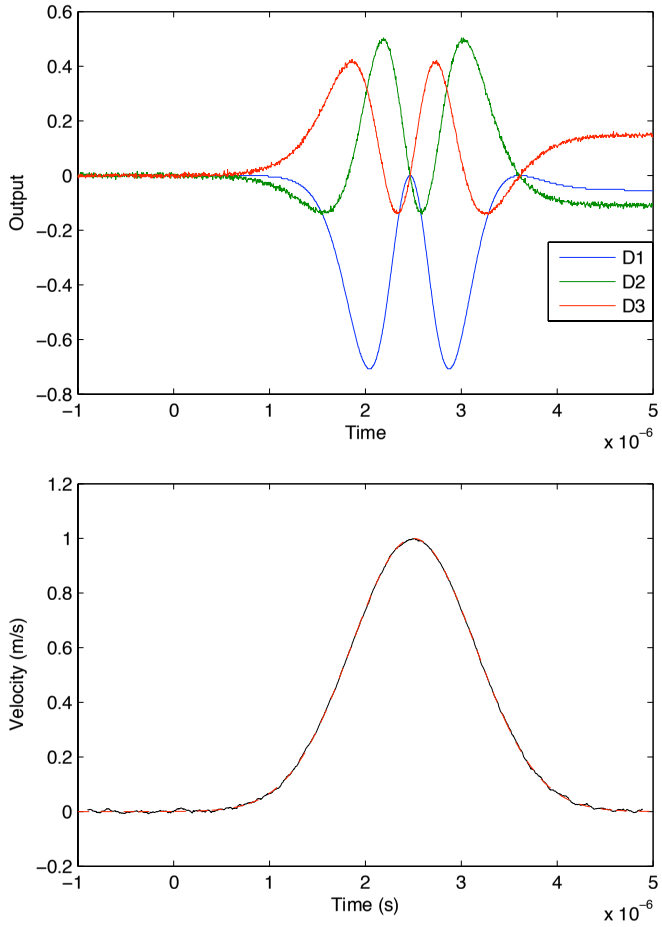

Figure 5.7. Imperfect measurement of a slow velocity pulse (benchmark problem C-2)

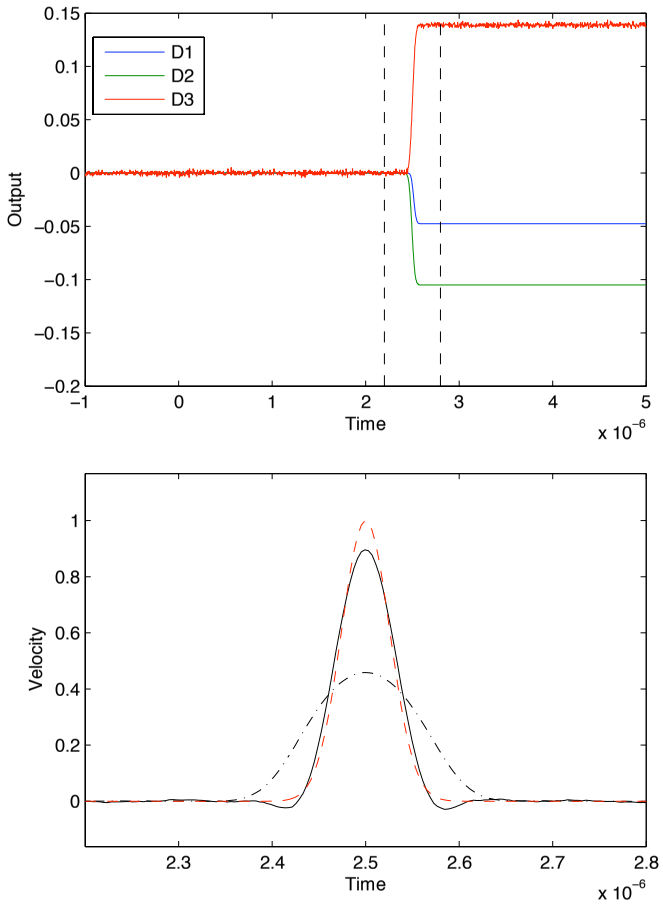

Figure 5.8. Imperfect measurement of a fast velocity pulse (benchmark problem C-4)

Proper analysis of benchmarks C-3 and C-4 is somewhat difficult since the data does not entirely span a complete ellipse. Noise-free data, such as C-3, is slightly more forgiving in this regard, but precise characterization utilizes data spanning no less that one half of an ellipse. To overcome this problem, one can perform ellipse characterization on benchmark problems C-1 and C-2, which share similar system characteristics, before loading the fast pulse data. This approach is similar to using characterization signals obtained prior to the measurement of interest (often on much slower time scales).

Users should be aware that the quadrature characterization on the "Quadrature signals" screen is not reliable in measurements spanning a small fraction of an ellipse. Since this characterization relies on an ellipse fit, partial ellipses may fool the program into thinking that the centering, aspect ratio, and quadrature error are far from their ideal state. However, if the analysis parameters on the previous screen (phase shift, R_{12}, etc.) are accurate, the calculated results will be correct.

CHAPTER 6

Summary

Three-phase measurements provide a method for extracting fringe shift in an interferometry measurement. The THRIVE program performs this reduction for both displacement and velocity interferometer configurations. A summary of the program features and plans for future releases are given below.

6.1 Program features

THRIVE accepts three-phase interferometer measurements from either a single text file or separate text files. Users may specify a characterization time range (over which signal characterization is performed) and an experiment time range (over which the analysis is performed). The signals may be reduced in either an ideal sense or by using ellipse characterization; the latter uses ellipse fits on signal pairs $D_1 - D_2$ and $D_1 - D_3$ to extract information about possible imperfections in the measurement. By default, THRIVE assumes all signals are DC coupled, but AC coupled signals are also supported.

The program uses a push-pull analysis to reduce three phase-shifted signals to an ideal pair of quadrature signals. With proper signal characterization, this reduction eliminates variable light conditions, imperfect phase shifts/splitting, and detector sensitivity from the measurement. The resulting fringe shift is used to calculate target position and velocity. The program utilizes Savitzky-Golay smoothing and differentiation to compensate for signal noise. Data generated by THRIVE can be exported to a text file for post-processing or saved in various graphical formats.

6.2 Future releases

Bug fixes will be made as necessary and will be distributed by electronic mail. Executable versions of THRIVE on OX X and Linux may be developed if there is user interest. Users should contact Daniel Dolan (`dhdolan@sandia.gov`) with bug reports and platform requests.

Features under consideration for future versions of THRIVE include:

- Binary file support in the "Load data" screen

- Capabilities for $> 10^7$ data points (64-bit operating systems only)
- Individual signal time shifting
- Recall of previous location and settings
- Analysis parameter archival in data export
- Beam-block characterization option

Feature requests should be sent to `dhdolan@sandia.gov`. No scheduled update to THRIVE is planned at this time, but new releases will be considered based on user feedback and developments in three-phase interferometry measurements.

References

[1] Barker, L. and Hollenbach, R. Laser interferometer for measuring high velocities of any reflecting surface. *Journal of Applied Physics* **43**, 4669–4675 (1972).

[2] Barker, L. Laser interferometry in shock-wave research. *Experimental Mechanics* **12**(5), 209 (1972).

[3] Strand, O., Goosman, D., Martinez, C., and Whitworth, T. Compact system for high-speed velocimetry using heterodyne techniques. *Review of Scientific Instruments* **77**, 83108 (2006).

[4] Dolan, D. Foundations of VISAR analysis. Technical Report SAND2006-1950, Sandia National Laboratories, (2006).

[5] Jensen, B., Holtkamp, D., Rigg, P., and Dolan, D. Accuracy limits and window corrections for photon Doppler velocimetry. *Journal of Applied Physics* **101**, 13523 (2007).

[6] Gabor, D. Theory of communication. *J. Inst. Electr. Engineering* **93**, 429 (1946).

[7] Hemsing, W. Velocity sensing interferometer (VISAR) modification. *Review of Scientific Instruments* **50**(1), 73 (1979).

[8] Weng, J., Tan, H., Hu, S., Ma, Y., and Wang, X. New all-fiber velocimeter. *Review of Scientific Instruments* **76**, 93301 (2005).

[9] Priest, R. Analysis of fiber interferometer utilizing 3×3 fiber coupler. *IEEE Transactions on Microwave Theory and Techniques* **MTT-30**(10), 1589 (1982).

[10] Dolan, D. and Jones, S. Push-pull analysis of photonic Doppler velocimetry measurements. *Review of Scientific Instruments* **78**(7), 076102 (2007).

[11] Choma, M., Yang, C., and Izatt, J. Instantaneous quadrature low-coherence interferometry with 3×3 fiber-optic couplers. *Optics Letters* **28**(22), 2162 (2003).

[12] Cheng, L., Koops, R., Wiedlers, A., and Ubachs, W. Develoment of a fringe sensor based on 3×3 fiber optic coupler for space interferometry. In *17th International Conference on Optical Fibre Sensors,* Voet, M., editor, volume 5855, 1004 (SPIE, Bellingham, WA, 2005).

[13] Savitzky, A. and Golay, M. Smoothing and differentiation of data by simplified least squares procedures. *Analytical Chemistry* **36**(8), 1627 (1964).

[14] Burden, R. and Faires, J. *Numerical Analysis.* PWS Publishing, Boston, 2nd edition, (1993).

[15] Halir, R. and Flusser, J. Numerically stable direct least squares fitting of ellipses. In *6th International Conference on Computer Graphics and Visualization,* Skala, V., editor, volume 1, 125–132 (University of West Bohemia Press, Plzen, Czech Republic, 1998).

[16] Press, W., Teukolsky, S., Vetterling, W., and Flannery, B. *Numerical Recipies in C: The Art of Scientific Computing.* Cambridge University Press, New York, 2nd edition, (1992).

DISTRIBUTION:

2 C. Doolittle
Applied Research Associates, Inc.
4300 San Mateo Blvd. NE
Suite A-200
Albuquerque, NM 87110

3 National Security Technologies
Los Alamos Operations
P.O. Box 809
Los Alamos, NM 87544
Attn: C. Gallegos
A. Iverson
V. Romero

2 National Security Technologies
Special Technologies Laboratory
5520 "B" Ekwill Street
Santa Barbara, CA 93111
Attn: B. Marshall
G. Stevens

2 Lawrence Livermore National Laboratory
7000 East Ave.
Livermore, CA 94550
Attn: O.T. Strand
T.L. Whitworth

6 Los Alamos National Laboratory
P.O. Box 1663
Los Alamos, NM 87545
Attn: M.R. Furlanetto
R.L. Gustavsen
W. Hemsing
D. Holtkamp
B.J. Jensen
P.A. Rigg

1	MS 1195	S.C. Alexander, 1647
1	MS 1195	T. Ao, 1646
1	MS 1195	J.R. Asay, 1646
2	MS 1159	J.W. Bryson, 1344
1	MS 1194	D.E. Bliss, 1644
1	MS 1195	J.-P. Davis, 1646
5	MS 1195	D.H. Dolan, 1646
1	MS 1195	M.D. Furnish, 1647
2	MS 1195	C.A. Hall, 1646
1	MS 1179	M.A. Hedemann, 1340

1	MS 1195	R.J. Hickman, 1646
5	MS 1159	S.C. Jones, 1344
1	MS 1195	M.D. Knudson, 1646
1	MS 1189	T.A. Mehlhorn, 1640
1	MS 1195	J.W. Podsednik, 1646
1	MS 1195	W.D. Reinhart, 1647
1	MS 1195	S. Root, 1646
1	MS 1195	T.F. Thornhill, 1647
1	MS 0834	W.M. Trott, 9112
1	MS 1195	T.J. Vogler, 1647
1	MS 1195	J.L. Wise, 1646
1	MS 0899	Technical Library, 9536 (electronic)


Sandia National Laboratories